Sub Topic: Droplets and Sprays

12th U. S. National Combustion Meeting
Organized by the Central States Section of the Combustion Institute
May 24–26, 2021 (Virtual)
College Station, Texas

Experimental combustion characteristics of n-butyl acetate synthesized by a new and sustainable biological process and comparisons with an ultrapure n-butyl acetate produced by Fischer esterification

*Yujie Wang[1], Zhu Chen[2], Matthew Haefner[1], Songtao Guo[1], Nicholas DiReda[1], Yuechao Ma[2], Yi Wang[2], C. Thomas Avedisian[1],**

[1]Sibley School of Mechanical and Aerospace Engineering
Cornell University, Ithaca, NY 14853
[2]Department of Biosystems Engineering
Auburn University, Auburn, AL 36849
**Corresponding Author Email: cta2@cornell.edu*

Abstract: Blending petroleum fuels with biofuels is a common approach for stemming the depletion of crude oil while also mitigating the impact of their combustion on the environment. It has recently been considered that n-butyl acetate (BA, $C_6H_{12}O_2$, boiling point of 399K) could be a viable biofuel additive to diesel fuel. This paper reports the combustion dynamics of BA droplets in the absence of external convection. Two grades of BA were examined: one synthesized by a new process that uses a solventogenic Clostridium strain through an extractive fermentation process using n-hexadecane as the extractant (SBA); the other commercially available as a high-purity (99.9%) 'neat' BA grade produced by Fischer esterification (NBA). The mass concentration of by-products from the synthesis process amounted to approximately 6% of the total composition and included n-butanol, n-hexadecane, iso-propyl alcohol and ethyl acetate. The platform used to study the combustion of commercial and synthesized BA was an isolated droplet burning with spherical symmetry. Initial droplet diameters were fixed at 0.6 mm. Experiments were carried out in a drop tower to promote one-dimensional transport dynamics, in the standard atmosphere, and with ignition accomplished by spark discharge. Differences in droplet burning rates and flame structures were undetectable between NBA and SBA, despite the differences in burning among the SBA components individually. The results presented show that the new synthesis process for butyl acetate yields a sustainable alternative to conventional methodologies with burning characteristics that are identical to NBA in stagnant gas transport fields.

Keywords: droplet combustion, n-butyl acetate, spherical symmetry, biofuel

1. Introduction

Biofuels have the potential to reduce the consumption of fossil fuels that power energy systems such as combustion engines. Blending biofuels with petroleum fuels (e.g., diesel, gasoline) is an effective way to realize a volumetric reduction of fossil fuels with generally favorable impacts on particulate and gaseous emissions. At the same time, biofuels typically have lower heats of combustion relative to petroleum fuels [1] and blending can reduce fuel economy.

Many biofuels have recently been considered as additives to petroleum fuels, and detailed screening processes have been developed for bioblendstocks (BOB) to aid in the selection [2-4]. Among the biofuels considered for blending with gasoline or diesel are esters. N-butyl acetate (BA; $C_6H_{12}O_2$, BP = 399K, MP=195K, ρL=885 kg/m3) in particular has favorable properties as a

sustainable biofuel additive to petroleum fuels, including considerations of freezing, boiling and flash points. As an oxygenated compound, BA shares with other biofuels a propensity to reduce (though not completely eliminate) particulate emissions through mechanisms based on carbon/oxygen bonds in the biofuel molecule which restrict carbon from becoming incorporated into soot [5].

BA is commonly produced via Fisher esterification. Conventional Fischer esterification consumes a large amount of energy and it is not necessarily environmentally friendly [6-8]. In comparison, production through biological routes can be renewable and environmentally friendly compared to fossil fuels [6,9]. Therefore, a sustainable method of production must be developed with the potential to produce BA, and in the quantities needed for the transportation sector. In 2019, this need would have been almost five billion gallons [10] for biofuel additives to diesel fuel at a 10% loading.

Moreover, BA's combustion performance - ignition, burn rate, particulate formation, etc. - is poorly understood. Two matters are addressed in this paper: a new process for producing BA, and the relationship between this new BA and a commercially available BA in terms of their combustion. While the emphasis of the present study is experimental, the combustion configuration used in the present study was selected to facilitate future modeling efforts. This is an important consideration for increasing the value of the data reported.

The BA synthesized by the new process described in this paper (i.e., synthesized butyl acetate, 'SBA') is compared with an ultrapure 'neat' grade of BA ('NBA') from Fischer esterification at 99.9% purity. It will not be unexpected for a biofuel synthesis process to yield dissolved by-products that render the BA produced a multicomponent miscible mixture highly diluted by BA. This potentiality would be the primary reason for observing differences between NBA and SBA.

2. Experimental methods

2.1 Fuel systems

The NBA used in the present work is a commercial product from Sigma-Aldrich (St. Louis, MO) with a stated purity of 99.9% (Sigma-Aldrich product number 442666-U). This is the benchmark grade for the comparisons reported in the present study.

For our new process, we have hypothesized [11] that clostridia could be an excellent microbial platform for BA production by taking advantage of its natural pathways for co-producing acyl-CoAs (acetyl-CoA and butyryl-CoA), fatty acids (acetate and butyrate), and alcohols (ethanol and butanol), either as intermediates or end-products. An efficient fatty acid ester production process was used to engineer comparatively high levels of BA through engineering a solventogenic Clostridium strain by an extractive fermentation process using n-hexadecane as the extractant. After fermentation, the liquid was purified through a distillation process that resulted in a mixture of NBA and the by-products listed in Table 1.

Table 1: SBA composition (property data from [12])

chemical →	NBA	n-butanol	n-hexadecane	iso-propanol	ethyl acetate	water	unknown
formula →	$C_6H_{12}O_2$	$C_4H_{10}O$	$C_{16}H_{34}$	C_3H_8O	$C_4H_8O_2$	H_2O	-
mass fraction	94.3%	3.8%	0.4%	0.134%	0.118%	0.865%	0.383%
boiling point	399 K	391 K	560 K	356 K	350 K	373 K	-
critical point	579 K	563 K	722 K	508 K	523 K	647 K	-

2.2. Droplet burning configuration

The configuration used to study SBA and NBA combustion is an isolated droplet burning under conditions that promote spherical droplet flames. Figure 1 is a schematic.

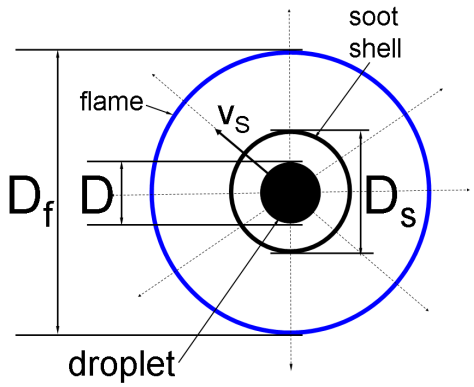

Figure 1: Schematic of idealized 1D droplet burning configuration.

The reason for choosing this configuration is that the SBA yield using the process noted in Section 2.1 is only several tens of milliliters at a time, which is insufficient for large scale testing in engines. The droplet configuration utilizes much smaller volumes, on the order of 10 µL. We do not expect SBA production at full scale, and therefore have selected the droplet configuration as appropriate for the fuel supplies we expect from our process. Moreover, the 1-D droplet configuration provides data on the evolution of droplet diameter (D) and flame diameter (D_f) as depicted in Figure 1 (though not soot shell diameter (D_s) in the case of BA) essential for detailed numerical modeling of droplet burning to validate numerical simulations and the associated fuel kinetic mechanisms. More commonly considered for such purposes over the droplet burning configuration are data from experimental configurations that pre-vaporize the fuel such as shock tubes, jet stirred reactors and other configurations that promote a 0-D or 1-D transport configuration to enable the application of detailed numerical models of gas-phase processes. Pre-vaporizing the fuel eliminates consideration of the liquid phase entirely and the droplet/gas coupling which is considered to influence kinetic mechanisms [13]. Droplet burning data complement these approaches and is relatively new in this application, as shown in several recent studies of different fuel systems [14-18].

2.3. Experimental setup

A brief description of the experimental design is provided in this section. Further details are given in [14,19]. The minimization of external convection to promote spherical droplet flames was achieved by anchoring test droplets at two intersecting 14 µm SiC fibers and eliminating buoyancy-induced and forced flows by carrying out the experiments in free-fall within a sealed chamber filled with air under standard conditions. Ignition was controlled by electrical discharges from two sparks positioned on opposite sides of the droplet and was initiated 200 ms after the package was released into free-fall. Spark duration was approximately 600 µs. The electrodes from which the sparks are formed were spring-loaded in solenoids to enable rapid retraction and precise re-positioning of the electrode tips after each experiment.

The droplet burning history was recorded by two cameras in perpendicular directions. One view provided backlit images from a high-speed black and white (BW) camera at 200 frames/s and 4MP per image, and the other provided color views of self-illuminated flames using a color

camera at 30 frames/s. The light source for the BW camera was provided by a single wavelength LED (Prismatix Mic-LED with BLCC-04; 637 nm). Quantitative data of droplet diameters were obtained from the video images using computer-based image analysis software [20]. Flame diameters were less sharp and were analyzed by a manual process using the ImagePro Plus (Rockville, MD, USA) software program. In the experiments reported, the initial droplet diameter was fixed at 0.6 mm with a precision of ±0.005 mm.

3. Results and discussion

3.1 Photographs of SBA and NBS droplet burning

Representative photographs of burning NBA and SBA droplets are shown in Figure 2 for burning without external convection. The time scale is in seconds because D_o was fixed precisely at 0.6 mm. Also shown in Figure 2 are representative photographs of the individual by-products of SBA listed in Table 1. The SBA and NBA photographs show no clear differences between their burning histories. The flame shapes are generally spherical throughout burning, which is expected because of the minimal effect of buoyancy and forced convection in the burning environment.

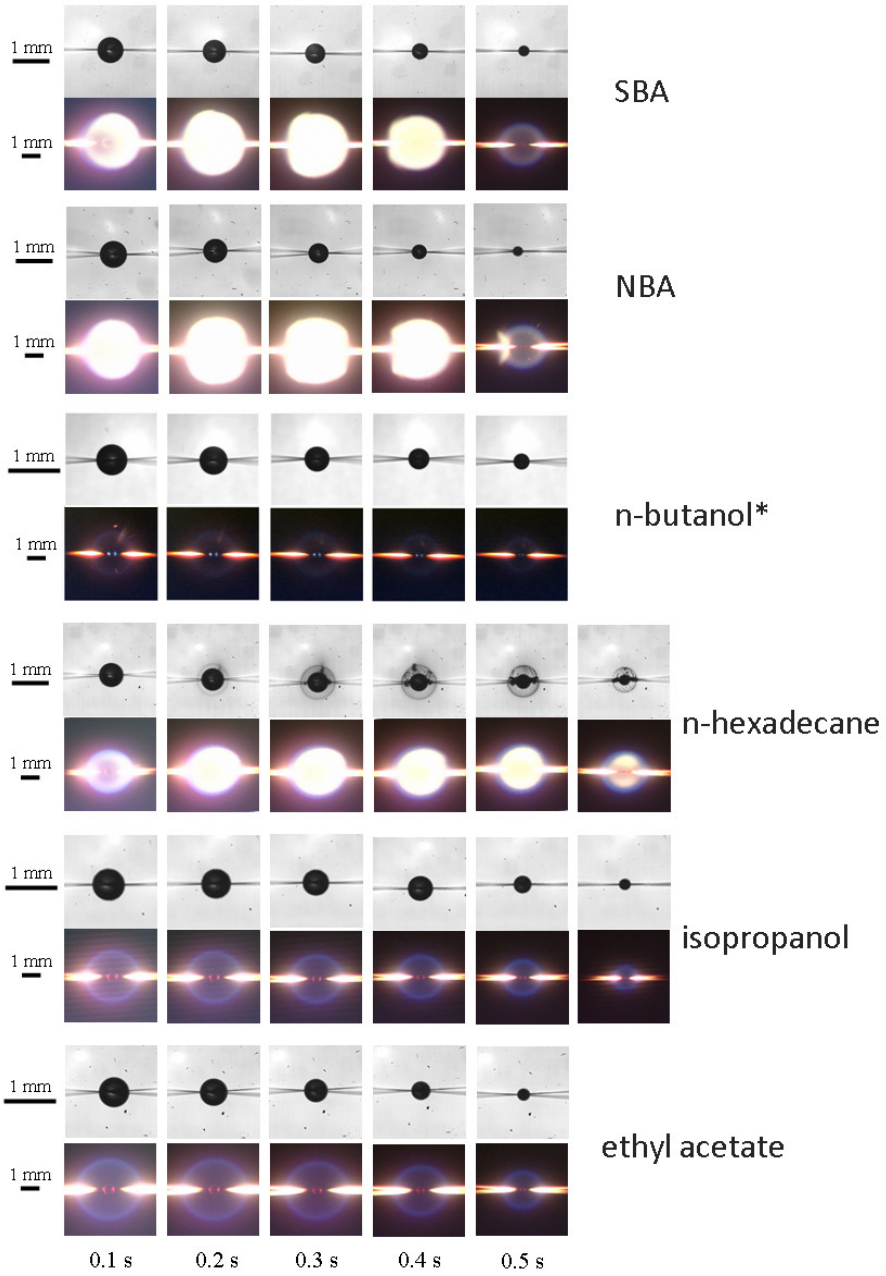

Figure 2: Time series images of the combustion of SBA and NBA, including the dissolved by-products of SBA, at 0.1 second intervals. *N-butanol results are from [21].

The luminosities of the SBA and NBA flames in Figure 2 show that soot has formed for these oxygenates, and the degree of flame luminosity is indicative of the amount of soot formed [22,23]. Of the SBA by-products in Table 1, hexadecane is the only one which has a sooting propensity high enough to where soot shells are visible. However, no soot shells are seen for SBA and NBA, so SBA flame luminosity cannot be attributed entirely to dissolved hexadecane. We speculate that the oxygenate in NBA delays the formation of soot aggregates to temperatures higher than the conventional soot inception temperature. With ignition closer to the high-temperature regions of the flame, ignited soot aggregates could burn up before a shell forms.

The bright lateral streaks in Figure 2 are due to the flame-fiber interaction. The direction in which the flame is viewed makes these streaks visible because the the glow along the fiber extends outside of the flame boundary. The flame appears to be stretched slightly in the lateral direction, which could be related to the flame anchoring mechanism for flame holders described in [24]. When the flame intersects the fiber, its temperature is high at that location and some distance away due to conduction in the fiber. Heat transfer from the fiber to the surrounding gas in contact with the fiber raises the gas temperature locally along the fiber. This gas preheating effect can enhance reaction rates, with the flame appearing to be extended out in the direction of the fiber.

Furthermore, the bright luminous zone gradually disappears during burning, which indicates reduced sooting as the droplet burns. This trend can be explained by the effect of droplet diameter on the residence time of fuel molecules transported between the droplet and the flame [25].

3.2 Quantitative measurements

The flame images shown in Figure 2 do not appear different to the naked eye, which is supported quantitatively by data confirming the similarity of NBA and SBA burning. For the evolution of droplet diameter, Figure 3a shows the evolution of droplet diameter in scaled coordinates for SBA and NBA. The absolute values of the slopes of these data provide the fuel burn rates. It is clear from this figure that SBA and NBA burn rates are practically identical. Similarly, the flame diameters expressed as the relative distance of the flame to the droplet in Figure 3b, D_f/D, are also virtually identical.

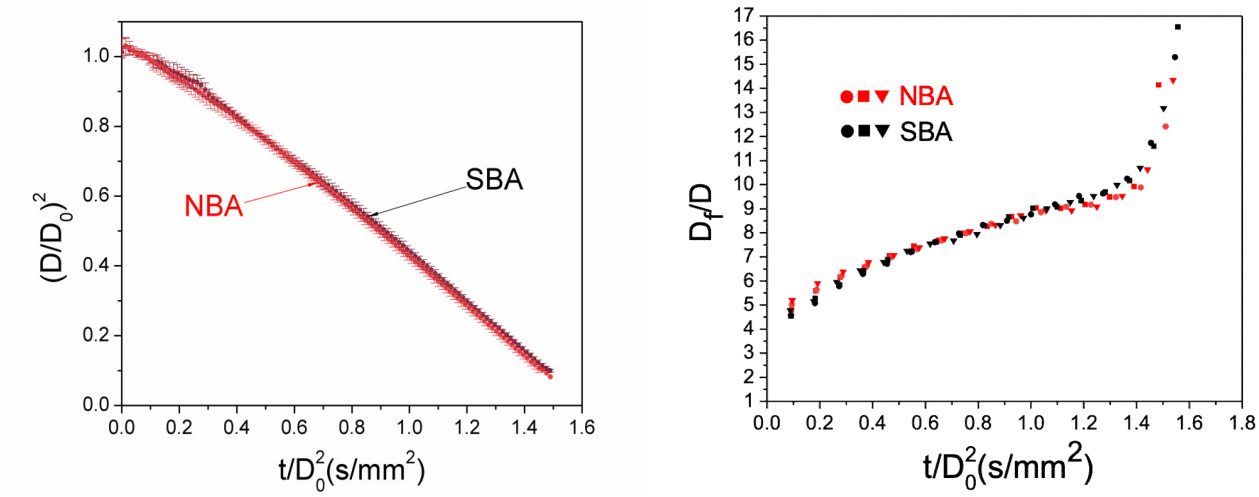

a) b)

Figure 3: a) Comparison of the evolution of averaged scaled droplet diameter with scaled time for NBA and SBA without convection; b) comparison of individual NBA and SBA data flame data, D_f/D, without convection.

Figure 3 further shows that the by-products in SBA do not have an influence on burning, likely because their mass concentration at 6% of the total composition is rather low. Additionally, the evolution of droplet and flame diameters in Figures 3a and 3b respectively also do not show any evidence of a preferential vaporization effect for SBA (it is not expected for NBA, which is 'pure'). Recent simulations [14] showed that multi-component droplets can exhibit a preferential vaporization effect even when more global features such as those in Figure

3 do not reveal this phenomenon, which emphasizes the value of detailed numerical modeling in providing an internal view of mixing and diffusion inside droplets. Unfortunately, for butyl acetate the lack of a detailed kinetic mechanism for its oxidation precludes such numerical modeling at the present time.

Figures 4a and 4b show the evolution of droplet diameter and the relative distance of the flame to the droplet for the SBA by-products respectively. The data are from individual experimental runs.

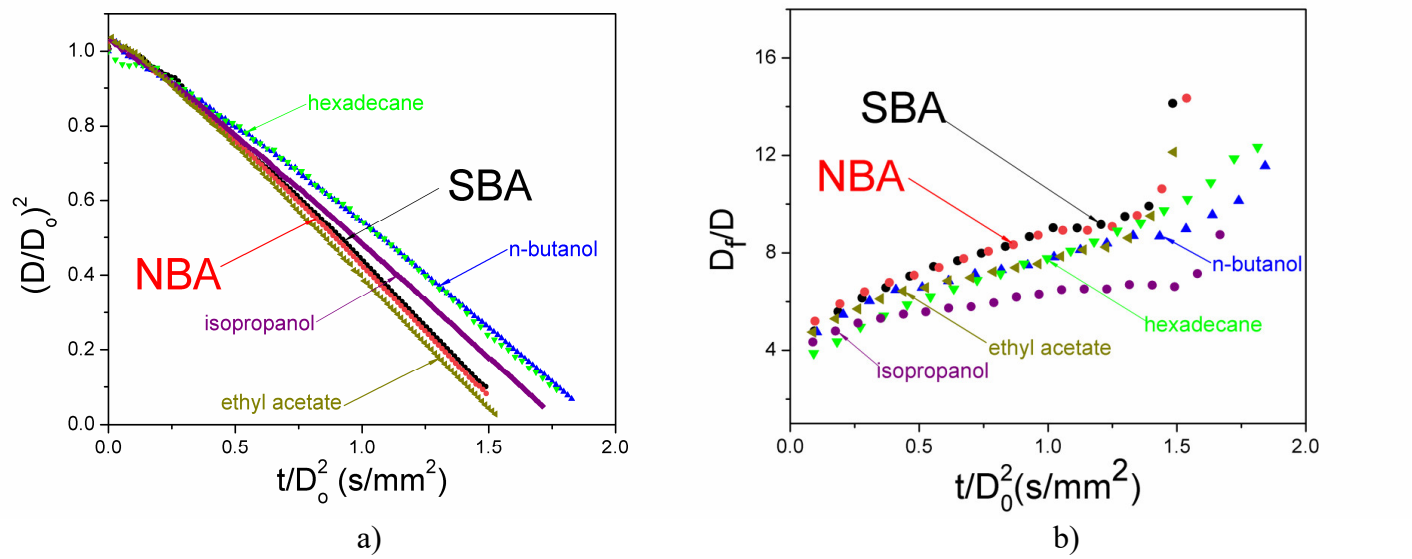

Figure 4: a) evolution of $(D/D_o)^2$ for SBA, NBA and SBA by-products without convection; b) evolution of relative position of flame to droplet diameter without convection.

Differences in the burning rates from Figure 4a are significant, with hexadecane and n-butanol burning the slowest and ethyl acetate the fastest and with a burning rate only slightly higher than SBA and NBA. Similarly, Figure 4b shows significant differences in flame positions among the SBA by-products, with all SBA by-products having flames closer to their droplet surfaces than the SBA flames are to the SBA droplet surface. Because SBA burns almost identically to NBA according to Figure 3, this perceived lack of an effect of the SBA by-products on SBA burning could be the result of a dilution effect from the low concentration of dissolved by-products, which suppresses their effect on burning.

4. Conclusion

The results presented show that synthesizing butyl acetate by a process that uses a solventogenic Clostridium strain through an extractive fermentation process using n-hexadecane as the extractant yielded a mixture of butyl acetate and dissolved by-products at just under 6% mass fraction. For burning under conditions that promoted spherical droplet flames through minimizing the influence of external convection, no discernable differences between the burning of SBA and NBA were identified. The droplet burning rates and flame structures were virtually identical between NBA and SBA though the individual by-product burning processes were different. No evidence of preferential vaporization was found for SBA though such an effect is not precluded. The study has shown that SBA is a viable alternative to butyl acetate produced by

conventional synthesis processes such as Fischer esterification.

5. Acknowledgements

The authors acknowledge helpful discussions with Drs. A.J. Agrawal and Josh Bittle of the University of Alabama. This work was supported in part by the US Department of Energy's Office of Energy Efficiency and Renewable Energy under Award number DE-EE0008483 with Dr Alicia Lindauer as the Program Manager. Additional support was received from the National Aeronautics and Space Administration (grants nos. NNX08AI51G and 80NSSC18K0480) with Dr. Michael C. Hicks as project monitor and DOE through award number DE-EE0007978.

6. References

[1] R.D.A. Andrade, E. Faria, A.M. Silva, W.C. Arauio, G.C. Jamie, K.P. Costa, A.G.S. Prado, Heat of combustion of biofuels mixed with fossil diesel oil, J. Thermal Analysis and Calorimetry 106 (2011) 469-474.

[2] R.L. McCormick, G. Fiorini, L. Fouts, E. Christensen, J.Yanowitz, E. Polikarpov, K. Albrecht, D.J. Gaspar, J. Gladden, A. George, Selection criteria and screening of potential biomass-derived streams as fuel blendstocks for advanced spark-ignition engines, SAE paper number 2017-01-0868 (2017).

[3] D.J. Gaspar, B.H. West, D. Ruddy, T.J. Wilke, E. Polikarpov, T.L. Alleman, A. George, E. Monroe, R.W. Davis, D. Vardon, A.D. Sutton, C.M. Moore, P.T. Benavides, J. Dunn, M.J. Biddy, S.B. Jones, M.D. Kass, M.M. Debusk, M. Sjoberg, J. Szybist, C.S. Sluder, G. Fioroni, W.J. Pitz, Top ten blendstocks derived from biomass for turbocharged spark ignition engines: bio-blendstocks with potential for highest engine efficiency, Report No. PNNL-28713, Pacific Northwest National Laboratory, 2019.

[4] P. Miles, Efficiency Merit Function for Spark Ignition Engines: Revisions and 1094 Improvements Based on FY16–17 Research, Report No. DOE/GO-102018-5041, 1095 U.S. Department of Energy. 2018. (see also https://www.nrel.gov/docs/fy18osti/67584.pdf).

[5] C.K. Westbrook, W.J. Pitz, H.J. Curran, Chemical Kinetic Modeling Study of the Effects of Oxygenated Hydrocarbons on Soot Emissions from Diesel Engines, Journal of Physical Chemistry A 110 (2006) 6912-6922.

[6] G. M. Rodriguez, Y. Tashiro, S. Atsumi, Expanding ester biosynthesis in Escher-ichia coli, Nature Chemical Biology 10(20144) 259-265.

[7] S. H. Ali, O. Al-Rashed, F.A. Azeez, S.Q. Merchant, Potential biofuel additive from renewable sources – Kinetic study of formation of butyl acetate by heterogeneously catalyzed transesterification of ethyl acetate with butanol, Bioresource Technology 102 (2011) 10094-10103.

[8] Y. Liu, E. Lotero, J.G. Goodwin, Effect of water on sulfuric acid catalyzed esterification, Journal of Molecular Catalysis A: Chemical 245 (2006) 132-140.

[9] C. Van den Berg, A.S. Heeres, L.A. van der Wielen, A.J. Straathof, Simultaneous clostridial fermentation, lipase-catalyzed esterification, and ester extraction to enrich diesel with butyl butyrate, Biotechnology and Bioengineering 110 (2013) 137-142.

[10] U.S. Energy Information Administration. Diesel fuel explained, see https://www.eia.gov/energyexplained/diesel-fuel/use-of-diesel.php, June 12, 2020

[11] J. Feng, J. Zhang, P. Wang, P. Jiménez-Bonilla, Y. Gu, J. Zhou, M. Cao, Z. Shao, I. Borovok, Y. Wang, Renewable Fatty Acid Ester Production in Clostridium, bioRxiv, 2020.03.29.014746.

[12] R.C. Reid, J.M. Prausnitz, B.E. Poling, The properties of gases and liquids, 4th edition,

McGraw-Hill, Boston, MA., 1987
[13] D. Haylett, P. Lappas, D. Davidson, R. Hanson, Application of an aerosol shock tube to the measurement of diesel ignition delay times, Proc. Combust. Inst. 32 (2009) 477-484.
[14] A. Cuoci, C. T. Avedisian, J.D. Brunson, S. Guo, A. Dalili, Y. Wang, M. Mehl, Alessio Frassoldati, K. Seshadri, J.E. Dec, D. Lopez-Pintor, Simulating combustion of a seven-component surrogate for a gasoline/ethanol blend including soot formation and comparison with experiments, Fuel 288 (2021) 119451.
[15] A. Dalili, J.D. Brunson, S. Guo, M. Turello, F. Pizzetti, L. Badiali, C.T. Avedisian, K. Seshadri, A. Cuoci, F.A. Williams, A. Frassoldati, M.C. Hicks, Experiments and Analysis of n-Heptane/Iso-butanol Droplet Combustion, Comb. Theory Modeling 24.6 (2020) 1002-1020 (2020)
[16] Y. C. Liu, F.E. Alam, Y. Xu, F.L. Dryer, C.T. Avedisian, T. Farouk, Combustion characteristics of butanol isomers in multiphase droplet configurations, Combust. Flame 169 (2016) 216-228.
[17] T. I. Farouk, Y.C. Liu, A,J,. Savas, C.T. Avedisian, F.L. Dryer, Sub-millimeter sized methyl butanoate droplet combustion: Microgravity experiments and detailed numerical modeling, Proc. Combust. Inst. 34 (2013) 1609-1616.
[18] Y.C. Liu, T.I. Farouk, A.J. Savas, F.L. Dryer, C.T. Avedisian, On the spherically symmetrical combustion of methyl decanoate droplets and comparisons with detailed numerical modeling, Combust. Flame 160 (2013) 641-655.
[19] Y.C. Liu, Y. Xu, M.C. Hicks, C.T. Avedisian, Comprehensive study of initial diameter effects and other observations on convection-free droplet combustion in the standard atmosphere for n-heptane, n-octane, and n-decane, Combust. Flame 171 (2016) 27-41.
[20] C.L. Dembia, Y.C. Liu, C.T. Avedisian, Automated data analysis of consecutive digital images from droplet combustion experiments by a MATLAB-based algorithm, Image Analysis and Stereology 31(2012) 137-148.
[21] Y. Xu, C.T. Avedisian, Combustion of n-butanol, gasoline, and n-butanol/gasoline mixture droplets, Energy & Fuels 29(20155) 3467-3475.
[22] C.J. Mueller and G.C. Martin, Effects of Oxygenated Compounds on Combustion and Soot Evolution in a DI Diesel Engine: Broadband Natural Luminosity Imaging, SAE paper number 2002-01-1631.
[23] I. Glassman, Combustion, 3rd ed., Academic Press, San Diego (1996), p. 270.
[24] J. Wan, H. Zhao, V. Akkerman, Anchoring mechanisms of a holder-stabilized premixed flame in a preheated mesoscale combustor, Phys. Fluids 32 (2020) 097103.
[25] G.S. Jackson, C.T. Avedisian, J.C. Yang, Observations of soot in droplet combustion at low gravity: heptane and heptane/monochloroalkane mixtures, Int. J. Heat Mass. Trans., 35.8 (1992), 2017-2033.